© 2014. Published by The Company of Biologists Ltd | Development (2014) 141, 4065-4075 doi:10.1242/dev.107987

RESEARCH ARTICLE

STEM CELLS AND REGENERATION

Quiescent neuronal progenitors are activated in the juvenile guinea pig lateral striatum and give rise to transient neurons

Federico Luzzati[1,2,*], Giulia Nato[1,2], Livio Oboti[1,2], Elisa Vigna[3], Chiara Rolando[2,4], Maria Armentano[2,5], Luca Bonfanti[2,5], Aldo Fasolo[1,2] and Paolo Peretto[1,2,*]

ABSTRACT

In the adult brain, active stem cells are a subset of astrocytes residing in the subventricular zone (SVZ) and the dentate gyrus (DG) of the hippocampus. Whether quiescent neuronal progenitors occur in other brain regions is unclear. Here, we describe a novel neurogenic system in the external capsule and lateral striatum (EC-LS) of the juvenile guinea pig that is quiescent at birth but becomes active around weaning. Activation of neurogenesis in this region was accompanied by the emergence of a neurogenic-like niche in the ventral EC characterized by chains of neuroblasts, intermediate-like progenitors and glial cells expressing markers of immature astrocytes. Like neurogenic astrocytes of the SVZ and DG, these latter cells showed a slow rate of proliferation and retained BrdU labeling for up to 65 days, suggesting that they are the primary progenitors of the EC-LS neurogenic system. Injections of GFP-tagged lentiviral vectors into the SVZ and the EC-LS of newborn animals confirmed that new LS neuroblasts originate from the activation of local progenitors and further supported their astroglial nature. Newborn EC-LS neurons existed transiently and did not contribute to neuronal addition or replacement. Nevertheless, they expressed Sp8 and showed strong tropism for white matter tracts, wherein they acquired complex morphologies. For these reasons, we propose that EC-LS neuroblasts represent a novel striatal cell type, possibly related to those populations of transient interneurons that regulate the development of fiber tracts during embryonic life.

KEY WORDS: Neural stem cells, Parenchymal progenitors, Postnatal neurogenesis, Internal capsule, Striatum, Transient neurons

INTRODUCTION

In the mammalian brain, a subset of neuronal progenitors (NPs) continues to produce neurons during postnatal and adult life. These cells are astrocytes residing in the subventricular zone (SVZ) and subgranular zone (SGZ) neurogenic niches, and give rise to olfactory bulb (OB) interneurons and dentate gyrus (DG) granule cells, respectively (Fuentealba et al., 2012; Ming and Song, 2011). The presence of quiescent NPs within other regions of the adult telencephalon has long been hypothesized (Emsley et al., 2005; Ourednik et al., 2001). NPs have been isolated *in vitro* from several non-neurogenic areas, particularly after invasive injuries (Buffo et al., 2008; Palmer et al., 1999), but it is unclear whether these progenitors only represent *in vitro* artifacts. Indeed, NPs generate mainly glial cells when transplanted into the mature brain parenchyma, thus leading to the idea that this environment is not permissive for neurogenesis during adulthood (Lim et al., 2000; Shihabuddin et al., 2000; Ninkovic and Götz, 2013).

However, low-level neurogenesis has been reported in several brain regions, such as the neocortex and striatum, of some mammalian species (Bonfanti and Peretto, 2011), and neurodegeneration strongly enhances such activity in rodents (Kernie and Parent, 2010). Newborn cortical and striatal neurons often exhibit a transient existence and, with few exceptions (Le Magueresse et al., 2011), their fate remains unclear or debated (Gould et al., 2001; Arvidsson et al., 2002; Chen et al., 2004; Dayer et al., 2005; Liu et al., 2009; Luzzati et al., 2011a; Ohira et al., 2010). Interestingly, in some cases these cells are generated by local parenchymal NPs. In the neocortex of adult rats, NPs are activated in layer I after mild ischemia (Ohira et al., 2010), and cortical GFAP$^+$ astrocytes have been shown to produce new neurons locally in perinatal mice under hypoxia/ischemia (Bi et al., 2011). In the striatum, we have identified local NPs generating new neurons under normal condition in rabbits, and during progressive neurodegeneration in mice (Luzzati et al., 2006, 2011a). In both mice and rabbits, striatal NPs showed features of intermediate NPs. Although these results support the contention that the mature striatal parenchyma can be permissive for the genesis of neurons, it remains to be clarified whether the observed NPs originate from the SVZ or from the activation of a local quiescent element.

Here, we demonstrate that the external capsule and lateral striatum (EC-LS) of the guinea pig contain local NPs that are quiescent at birth and become activated during postnatal development, peaking at weaning. Newborn striatal neurons in the guinea pig exist transiently and do not express markers of striatal neurons, yet they might be involved in a transient form of plasticity.

RESULTS

DCX$^+$ neuroblasts in the juvenile guinea pig EC-LS

In the juvenile guinea pig a population of DCX-labeled cells is visible in the ventral half of the EC and the surrounding parenchyma of the LS (Fig. 1A,D) (Luzzati et al., 2011b). All the DCX$^+$ cells in the EC-LS expressed the neuronal marker Tuj1 (Fig. 1E,F), but not the oligodendrocyte markers Olig2 and SOX10 (not shown), or the astrocyte marker GFAP (Fig. 2C), indicating they belong to the neuronal lineage. At p18, the distribution of the DCX$^+$ cells spans ~4-5 mm along the EC-LS, rostral to the decussation of the anterior commissure. This system is always anatomically separated from the SVZ (Fig. 2A). In the more ventral part of the EC, the DCX$^+$ cells were mostly organized in large chains, oriented parallel to the EC fibers and closely associated to blood vessels (Fig. 1C; supplementary material Fig. S1). Here, we will refer to this ventral part of the EC as the ventral pallial-subpallial boundary (vPSB; Fig. 1D). In contrast to

[1]Department of Life Sciences and Systems Biology (DBIOS), University of Turin, Turin 10123, Italy. [2]Neuroscience Institute Cavalieri Ottolenghi (NICO), Orbassano 10010, Italy. [3]Department of Oncology, University of Turin, c/o Institute for Cancer Research and Treatment (IRCC), Candiolo 10060, Italy. [4]Department of Neuroscience, University of Turin, Turin 10126, Italy. [5]Department of Veterinary Sciences, University of Turin, Grugliasco 10095, Italy.

*Authors for correspondence (federico.luzzati@unito.it; paolo.peretto@unito.it)

Received 17 January 2014; Accepted 27 August 2014

Development (2014) 141, 4065-4075 doi:10.1242/dev.107987

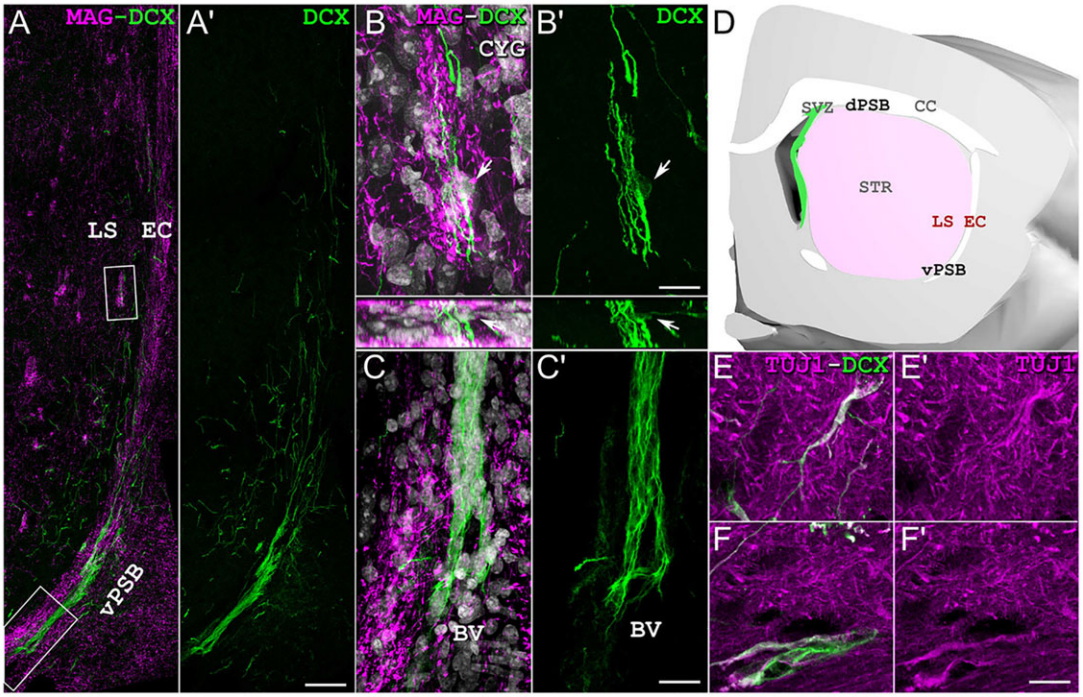

Fig. 1. DCX$^+$ neuroblasts in the EC-LS of the juvenile guinea pig. (A,A′) Coronal section stained for myelin associated glycoprotein (MAG; magenta), DCX (green) and with nuclear stain (Cytox Green, CYG; white). (B-C′) Higher magnifications of boxed regions in A showing a cell body (arrow) and processes of individual DCX$^+$ cells within an IC bundle (B), and a chain of DCX$^+$ neuroblasts running along a blood vessel in the vPSB; lower panel in B,B′ shows an *x,z* view of the stack. (D) Schematic of the guinea pig striatum (coronal view). (E-F′) Both individual DCX$^+$ (green) cells (E) and chains (F) express the neuronal marker Tuj1 (magenta). BV, blood vessel; CC, corpus callosum; LS, lateral striatum; EC, external capsule; d/vPSB, dorsal/ventral pallial-subpallial border; STR, striatum; SVZ, subventricular zone. Scale bars: 40 µm in A,A′; 15 µm in B,B′; 10 µm in C,C′,E-F′.

the vPSB, in the dorsal EC and in the LS DCX$^+$ cells were exclusively represented by individual elements, often located within the white matter tracts of EC and internal capsule (IC; Fig. 1B). Interestingly, the vPSB was highly enriched in astrocytes that, like neurogenic astrocytes of the embryonic and adult neurogenic niches, expressed GFAP (Doetsch et al., 1999; Garcia et al., 2004), BLBP (Anthony et al., 2004; Giachino et al., 2013), Vimentin (Doetsch et al., 1999; Schnitzer et al., 1981) and PAX6 (Götz et al., 1998; Maekawa et al., 2005) (Fig. 2B,C; supplementary material Fig. S2; data not shown). Ultrastructural analyses of the vPSB at postnatal day (p) 18 confirmed the presence of clusters of small cells showing characteristics typical of neuroblasts: immunoelectrondense cytoplasm filled with free ribosomes, scarce endoplasmic reticulum and darkly stained nuclei (Fig. 2D). These cells form chain-like structures that are in contact with unmyelinated and myelinated axons, abundant astrocytic processes and, in some cases, blood vessels.

Overall, these data support the occurrence of an SVZ-independent neurogenic niche in the vPSB of the juvenile guinea pig. Similar to the SVZ-OB system, the vPSB chains might represent early stages of the neurogenic process, which are followed by the detachment of individual cells migrating toward the dorsal EC and LS.

Development of the EC-LS neurogenic system

To better characterize the EC-LS neurogenic system, we followed its postnatal development. Note that, in contrast to mouse, rat and rabbit, the guinea pig is a highly precocial mammal. Newborns have teeth, fully grown fur and well developed sensory and locomotor abilities (Künkele and Trillmich, 1997).

There were very few DCX$^+$ cells in the EC-LS at birth (176±46 cells, n=3) and their number was not significantly changed at p7 (460±129 cells, n=3; one-way ANOVA, F=35,09; Tukey's post-hoc p1 versus p7, P=0.99; Fig. 3A,E,H). By contrast, these cells increased abruptly between p7 and p18 (5440±1355 cells at p18, n=3; p7 versus p18, P<0.0001; Fig. 3A,F,I), then declined gradually, being reduced to about half by p50 (p18 versus p50, P=0.003) and almost absent at 8 months of age (p18 versus p240, P<0.0001; Fig. 3A,G,J).

The proportion of DCX$^+$ cells organized in chains or as individual elements was similar at all ages, with the exception of p1 animals, in which no chains were visible (Fig. 3A,E,H), supporting a direct relationship between chains and individual elements, at least by p7. At all ages, strong DCX immunolabeling was found in the SVZ and DG indicating that the trend in DCX expression found in the EC-LS is not due to age-dependent variations in immunoreactivity for DCX (Fig. 3B-D).

To further analyze the differential abundance of neuroblasts during postnatal development, we cultured explants of the SVZ and EC-LS from p1 and p18 animals (supplementary material Fig. S3). Consistent with previous studies in other species (Lois and Alvarez-Buylla, 1993; Luzzati et al., 2006), numerous DCX$^+$ cells migrated out of both p1 and p18 SVZ explants after 3 days *in vitro* (supplementary material Fig. S3A,B). By contrast, the EC-LS explants were surrounded by very few DCX$^+$ cells at p1, whereas at p18 the number of DCX$^+$ neuroblasts increased ~20-fold (52±55 DCX$^+$ cells at p1 versus 1022±286 DCX$^+$ cells at p18, n=4 animals per group; t-test, P=0.001; supplementary material Fig. S3C,D,F).

Collectively, these data indicate that the EC-LS DCX$^+$ cells are mostly associated with a specific developmental window that spans from the weaning period (p18) to the peri-pubertal age (p50).

EC-LS neuroblasts are mostly generated between p7 and p18

To establish the rate of genesis of the DCX$^+$ cells in the EC-LS during postnatal development, BrdU was given at p1, p7 and p18,

Development (2014) 141, 4065-4075 doi:10.1242/dev.107987

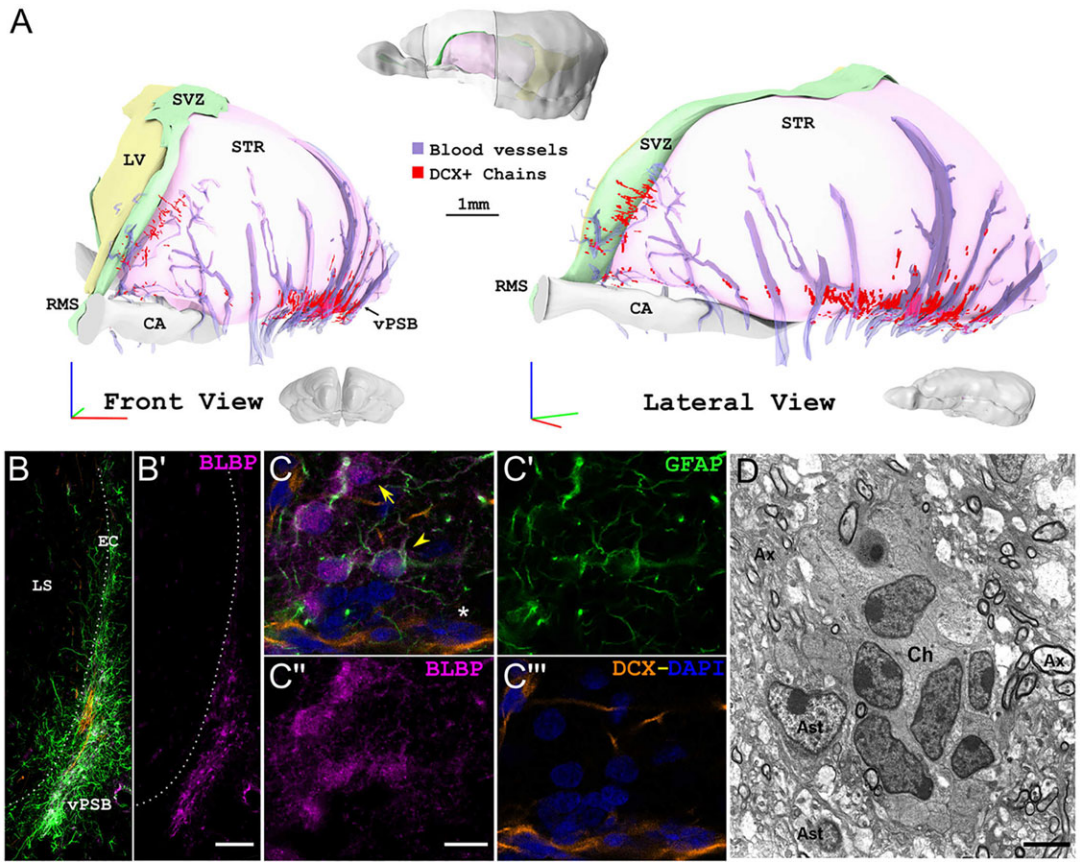

Fig. 2. Anatomical and cellular organization of the EC-LS neurogenic system. (A) Frontal (left) and lateral (right) views of a 3D model obtained from DCX-stained coronal sections. The location of the reconstructed region is outlined in the central model. DCX$^+$ chains (red) are mostly restricted to the vPSB and in close contact with blood vessels (violet). (B-C‴) Coronal section at the level of the vPSB labeled with GFAP (green), BLBP (magenta), DCX (orange) and DAPI (blue in C). (C) A single confocal plane showing GFAP/BLBP co-expression (arrowhead). As BLBP labels mainly the cell body, whereas GFAP labels the processes, colocalization is often ambiguous (arrow). The asterisk marks a DCX+ but GFAP– and BLBP– neuroblast. (D) Ultrastructural analysis of vPSB. Small cells are observed with the typical feature of neuroblasts forming a chain (Ch) and contacting axons (Ax), astrocytes (Ast) and astrocytic processes (recognizable by their white cytoplasm). CA, anterior commissure; RMS, rostral migratory stream. Scale bars: 1 mm in A; 300 µm in B-C‴; 3 µm in D.

and the animals sacrificed 11 days after the injection (n=4 animals per group; Fig. 4G). In p1 and p7 injected animals, only very few DCX$^+$/BrdU$^+$ colabeled elements were found (p1, 44±12 cells; p7, 222±149 cells; one-way ANOVA, F=16,3, P=0.004; Tukey's post-hoc, P=0.658), whereas in animals treated at p18 these cells were dramatically increased (p18, 1096±390 cells; Tukey's post-hoc p7 versus p18, P=0.004; n=4; Fig. 4A-E,G). This indicates that EC-LS neuroblasts are mostly generated between p7 and p18.

At all survival times considered, the DCX$^+$/BrdU$^+$ cells were found both as individual elements, homogeneously distributed among the EC and LS (Fig. 4A-C), and in vPSB chains (Fig. 4D,E). Note that although the density of BrdU$^+$ cells in the LS increased between p1 and p18 (t-test, P=0.020), this increase involved only the DCX$^+$ cells (P=0.021), since no variation in cell density was found for BrdU$^+$/SOX10$^+$ oligodendrocytes (P=0.111), or in those BrdU$^+$ cells not expressing DCX or SOX10 (P=0.195; Fig. 4F,H). Thus, in contrast to the SVZ and DG, in which neurogenesis begins during embryonic development (Kriegstein and Alvarez-Buylla, 2009), in the EC-LS of the guinea pig neurogenesis is activated during postnatal development.

Induction of neurogenesis in the vPSB is associated with the appearance of primary and intermediate-like NPs

The presence of chains of neuroblasts surrounded by cells showing features of neurogenic astrocytes (Fig. 2B-D) is consistent with the occurrence of a neurogenic niche in the vPSB. To test this possibility, we first analyzed the density and distribution of EC-LS cells expressing the marker of proliferation Ki67 (Scholzen and Gerdes, 2000). Between p1 and p18 the density of Ki67$^+$ cells remained constant in the LS (t-test, P=0.333) and dorsal EC (P=0.125), whereas it strongly increased in the vPSB (P=0.004; n=3; Fig. 5A,B,I). This increase was mostly due to the appearance of Ki67$^+$ cells organized in clusters (Fig. 5C), which represent 68±11% of all the Ki67$^+$ cells in the vPSB at p18. 60.9±4.1% of the clustered Ki67$^+$ cells expressed DCX, and 89.3±5.3% of these double-labeled cells were part of a DCX$^+$ chain (n=3). These results show that the Ki67$^+$ clusters and the DCX$^+$ chains are closely associated and partly overlapping structures. A 2 h pulse of BrdU confirmed that the clustered Ki67$^+$ cells of the vPSB were actually proliferating (Fig. 5E).

Among the Ki67$^+$ clusters containing at least one DCX$^+$ cell, 24.32±6.61% of the cells did not express DCX (n=3). We refer to these cells as Ki67$^+$ cells associated with proliferating neuroblasts, or KaD cells (Fig. 5D). The clustered arrangement, together with the lack of DCX expression suggest that the KaD cells might represent intermediate NPs (Fuentealba et al., 2012). Accordingly, in contrast to the postmitotic (DCX$^+$/Ki67$^-$) neuroblasts the DCX$^+$/Ki67$^+$ and KaD cells strongly expressed PAX6 (Fig. 5F,H) and SOX9 (not shown), two markers that characterize the SVZ intermediate NPs (Cheng et al., 2009; Hack et al., 2005; Kohwi et al., 2005).

Development (2014) 141, 4065-4075 doi:10.1242/dev.107987

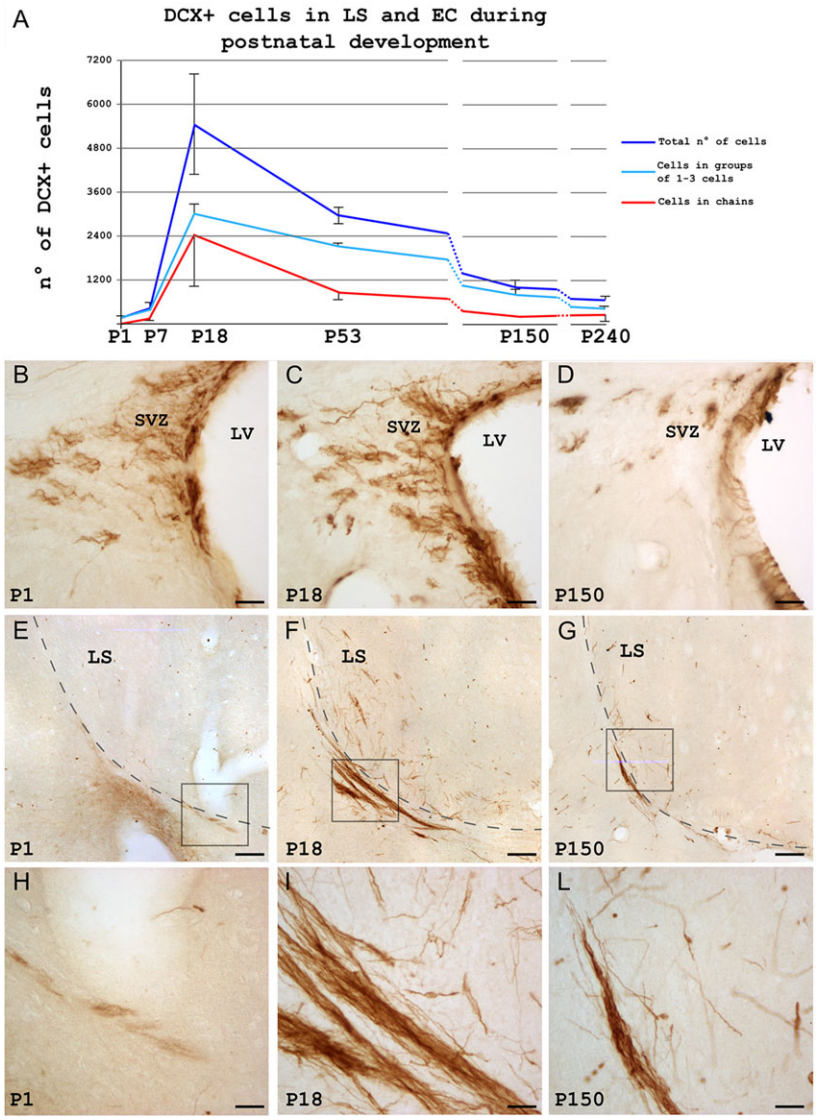

Fig. 3. Timecourse analysis of the DCX$^+$ cells in the EC-LS during postnatal development. (A) Stereological estimates of the mean±s.d. number of DCX$^+$ cells (blue line) in the EC-LS at different postnatal ages. Red and cyan lines indicate cells organized in chains or as individual elements. (B-J) DCX expression in SVZ (B-D) and EC-LS (E-J) at p1 (B,E,H), p18 (C,F,I) and p150 (D,G,J). (H-J) Higher magnifications of the boxed regions in E-G. Dashed line (E-G) indicates the border between LS and EC. Scale bars: 100 µm in E-G; 25 µm B-D,H-J.

Interestingly, the appearance of intermediate-like NPs between p1 and p18 was accompanied by a steep increase in BLBP$^+$ cells that expressed Ki67 in the vPSB (P=0.003; Fig. 5G,J). The astrocytic nature of the vPSB BLBP$^+$ cells was consistent with their predominant co-expression of GFAP, but not DCX (Fig. 2C) or SOX10 (Fig. 5G). By contrast, the Ki67$^+$/SOX10$^+$ oligodendrocyte progenitors (Fig. 5G) showed only a small tendency to increase in the vPSB at p18 (P=0.077; Fig. 5K). Like the primary progenitors of other neurogenic niches (Ponti et al., 2013), vPSB BLBP$^+$ cells were rarely proliferating, representing only 3.7±1.8% of all Ki67$^+$ cells at p18 (n=3). To determine whether these are label-retaining cells, we injected BrdU for 5 consecutive days from p18 and analyzed the animals either 15 (15 d) or 65 (65 d) days after the first injection. Although the total number of BrdU$^+$ cells dropped between 15 d and 65 d (15 d, 1745±150 cells/mm^2; 65 d, 265±40 cells/mm^2; t-test, P=0.002; n=3), those expressing BLBP showed a more moderate decrease (15 d, 80±7 cells/mm^2; 65 d, 45±8 cells/mm^2; P=0.003). Accordingly, only 4.4±0.3% of BrdU$^+$ cells expressed BLBP in the vPSB at 15 d, but this value increased to 16.8±1.8% at 65 d (P=0.007). At both time points the BLBP$^+$/BrdU$^+$ cells were at least in part colabeled for GFAP (Fig. 6; data not shown), confirming their astrocytic nature. Thus, by p18, vPSB astrocytes become proliferative and retain BrdU labeling long-term, further supporting the contention that they include primary NPs.

Overall, these data indicate that the occurrence of immature neuroblasts in the EC-LS correlates with the appearance of cells showing features of both primary and intermediate NPs.

To further confirm the occurrence of local NPs in the EC-LS, after a 2 h BrdU pulse *in vivo* we performed tissue explants of the EC-LS and SVZ from p18 animals. Double staining for DCX and BrdU showed several colabeled cells surrounding both the SVZ and EC-LS explants (n=3; Fig. 7). Interestingly, DCX$^+$/BrdU$^+$ cells were also identified in EC-LS and SVZ cultures when BrdU was added to the culture medium for 24 and 48 h starting from the second day *in vitro* (n=2; Fig. 7C). These data indicate that, at p18, the EC-LS of the guinea pig contains active NPs.

EC-LS NPs derive from the activation of local cells

Two non-mutually exclusive hypotheses can be drawn regarding the origin of the vPSB NPs: (1) they migrate from already active neurogenic niches (i.e. the SVZ); (2) they are local cells that become active around weaning. To investigate this, we injected newborn animals with a GFP-tagged lentiviral vector in the SVZ or in the EC-LS. In addition, to determine whether infected cells behave as NPs later in development, a group of animals was treated with BrdU at p18 for 5 consecutive days (50 mg/kg, one intraperitoneal injection/day) and left to survive for a further 15 days until p33 (Fig. 8A).

Development (2014) 141, 4065-4075 doi:10.1242/dev.107987

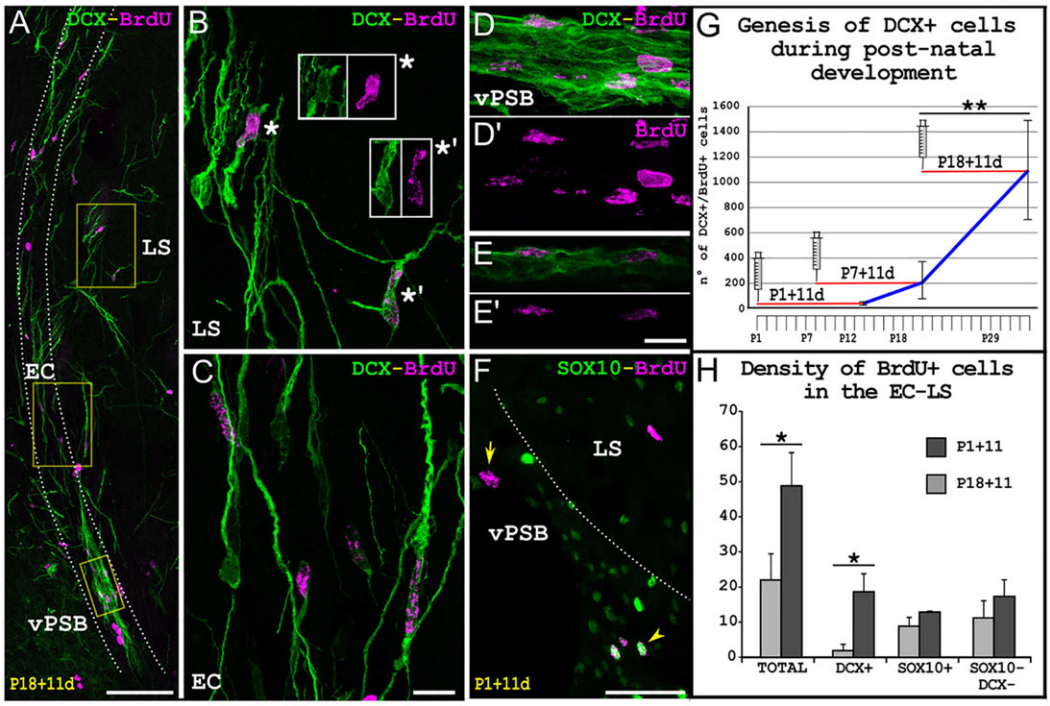

Fig. 4. Rate of cell genesis in the EC-LS during postnatal development. (A) Section of EC-LS stained for DCX (green) and BrdU (magenta) in a p29 animal injected with BrdU at p18 (p18+11d). (B-D′) Higher magnifications of the boxed regions in A. In B, single confocal planes of the cells marked by asterisk and asterisk with prime are shown in the insets. (E,E′) Single confocal plane of the chains in D. (F) Coronal section from a p12 animal injected with BrdU at p1 (p1+11) showing BrdU$^+$ cells (magenta) that are either SOX10$^+$ (arrowhead) or SOX10$^-$ (arrow). (G) Number of DCX/BrdU colabeled cells in the EC-LS at different postnatal ages (blue line). The red lines indicate the survival time. (H) Density of total BrdU$^+$ cells and of BrdU$^+$ cells that are DCX$^+$, SOX10$^+$ or DCX$^-$/SOX10$^-$ in the EC-LS between p1 and p18. Error bars indicate s.d. *P<0.05, **P<0.005 (G, one-way ANOVA; H, t-test). Scale bars: 75 µm in A,F; 10 µm in B-E′.

When the VSVG-GFP virus was injected in the lateral ventricle, GFP-labeled cells were observed over the entire SVZ up to the olfactory ventricle. Many of these cells had an astrocytic-like morphology (Fig. 9A; data not shown). In addition, GFP labeling was also found in the migrating neuroblasts of the RMS, often colabeled with BrdU (Fig. 9B), as well as in the deep and superficial granules and periglomerular cells of both main (Fig. 9B-D) and accessory OB, indicating that VSVG-GFP targeted primary SVZ progenitors over multiple domains (Merkle et al. 2007). In the six analyzed hemispheres we estimated a total of 3588 GFP$^+$ cells in the OB, whereas we never observed any GFP-labeled cells in the EC-LS, suggesting that the SVZ does not contribute to the EC-LS neurogenic system.

In order to label the vPSB, we took advantage of the fact that this region is supplied by numerous large veins that drain the striatum (Fig. 2A); thus, we injected VSVG-GFP in the dorsolateral caudate putamen (Fig. 10A,B). At 3 days post-infection a very strong GFP labeling was evident at both the injection site and in the vPSB, whereas only rare GFP$^+$ cells were visible in the LS (Fig. 10C) and dorsal EC (n=7 hemispheres from five animals). Surprisingly, at this time GFP expression in the vPSB cells was found mainly associated with BLBP$^+$ astrocytes (82.3±11.2%), and to a much lesser extent with NeuN$^+$ neurons (8.2±3.9%) and SOX10$^+$ oligodendrocytes (4.6±2.2%). At p33, a considerable proportion of DCX$^+$ cells of the LS and dorsal EC expressed GFP [19.6-39.7%; mean±s.d. of DCX$^+$/GFP$^+$ cells among DCX$^+$ cells: 30.8±7.3% (187 DCX$^+$/GFP$^+$ among 602 DCX$^+$ cells counted in four animals; number of DCX$^+$/GFP$^+$ cells ranged from 30 to 83 per animal)]. The morphology and distribution of GFP$^+$ and GFP$^-$ neuroblasts in the EC and LS were not evidently different (Fig. 10E). 33.8±7.3% of DCX$^+$/GFP$^+$ cells incorporated BrdU (63 DCX$^+$/GFP$^+$/BrdU$^+$ cells in four animals; Fig. 10F). Notably, this percentage was the same as that of BrdU$^+$ cells among DCX$^+$/GFP$^-$ cells (27.1±6.3%; t-test, P=0.266). Thus, vPSB cells infected at p1 can behave as NPs at p18, giving rise to a progeny that is virtually identical to that of uninfected progenitors. These data indicate that the EC-LS neurogenic system involves the activation of local quiescent NPs and further suggest that these cells are BLBP$^+$ astrocytes.

Neuroblasts generated in the EC-LS exist transiently and belong to a novel neuronal type

To investigate the fate of DCX$^+$ neuroblasts, we performed a BrdU timecourse analysis in animals that received BrdU for 5 consecutive days, starting at p18 (Fig. 8B). The number of BrdU$^+$/DCX$^+$ cells in the LS and EC dropped between 15 and 35 days from the first BrdU injection (t-test, P=0.01), and these cells disappeared by 65 days (Fig. 11A). At all survival times, BrdU$^+$ cells did not express markers of known striatal neurons [DARPP-32, Calbindin, Parvalbumin, Calretinin, nNOS, ChAT (Kawaguchi, 1997)] or transcription factors involved in their differentiation [Isl1, Nkx2.1 (Marin et al., 2000)]. Thus, newborn DCX$^+$ cells of the EC-LS may either die or differentiate into a neuronal type that does not express conventional striatal markers. To analyze this possibility, we traced the vPSB cells by injection of a GFP lentiviral vector at p14. Between p18 and p26, the animals were treated with six BrdU injections, and then sacrificed 30 days after the last injection (Fig. 8C; n=4). In the LS and dorsal EC of these animals (one in three sections/animal) we identified 56 GFP$^+$/BrdU$^+$ cells (Fig. 11B) and only two of them were negative for DCX (3.6% of all GFP$^+$/BrdU$^+$; not shown). Notably, in the vPSB we always found some GFP$^+$ cells showing morphologic features of astrocytes and that expressed BLBP and were BrdU$^+$ (Fig. 11E-H), indicating that VSVG-GFP-infected vPSB BLBP$^+$ cells were able to proliferate and retain BrdU labeling long-term. Except for the

Development (2014) 141, 4065-4075 doi:10.1242/dev.107987

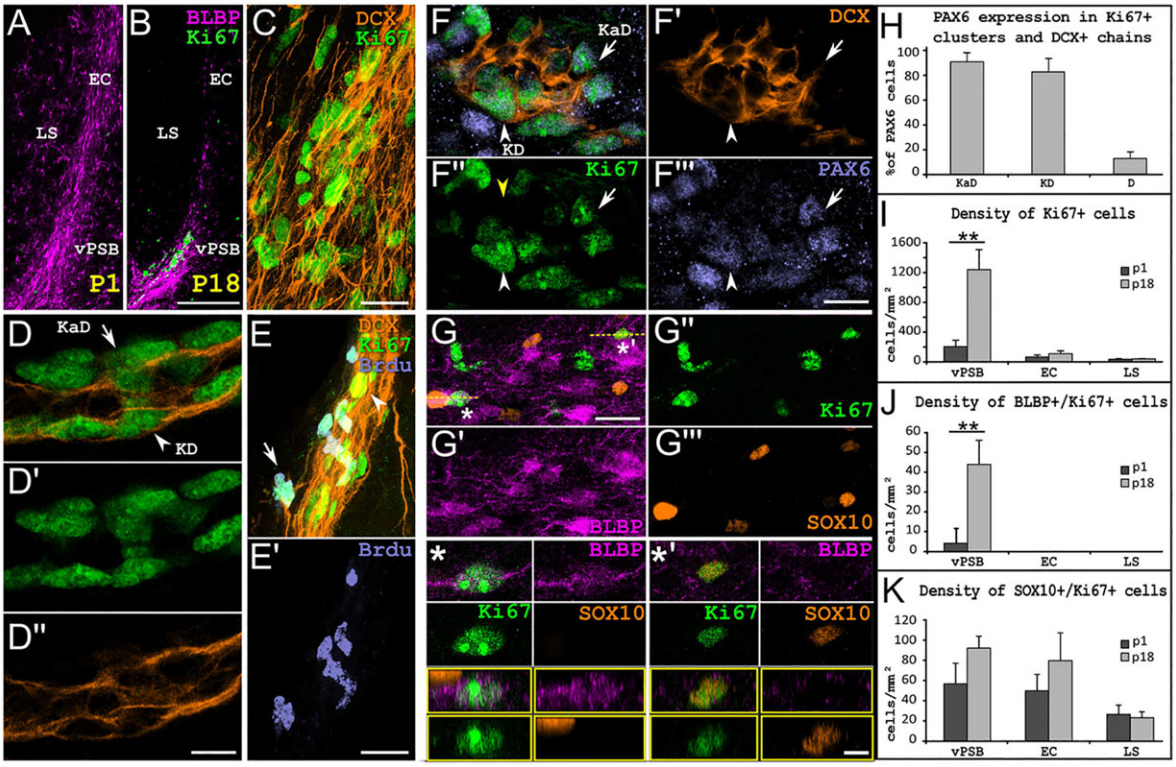

Fig. 5. Ki67$^+$ cells in the EC-LS during postnatal development. (A,B) Coronal sections of the EC-LS from p1 (A) and p18 (B) animals stained for BLBP (magenta) and Ki67 (green). (C) Clusters of Ki67$^+$ cells (green) closely associated with DCX$^+$ chains (orange). (D-D″) Single confocal plane showing Ki67$^+$ cells that in part express DCX (KD arrowheads) and in part do not (KaD arrow). (E,E′) Ki67$^+$ cells that express (arrowheads) or do not express (arrow) DCX are labeled by a 2 h BrdU (violet) pulse in the vPSB at p18. (F-F‴) Single confocal plane showing the colocalization of PAX6 (violet) and Ki67 in both KaD (arrow) and KD (arrowhead) cells in the vPSB at p18. (G-G‴) Colabeling between Ki67 and BLBP (magenta, asterisk) or SOX10 (orange, asterisk with prime) in the vPSB at p18. A single confocal plane and a reslice (yellow outline) along the yellow line in G is shown for both cells. (H-K) The percentage of KaD, KD and D cells co-expressing PAX6 (H) and the density of Ki67$^+$ (I), BLBP$^+$/Ki67$^+$ (J) and SOX10$^+$/Ki67$^+$ (K) cells in the vPSB, EC and LS, between p1 and p18. Error bars indicate s.d. $^{**}P$<0.005 (*t*-test). Scale bars: 100 µm in A,B; 20 µm in C,E,E′,G-G‴; 10 µm in F-F‴; 5 µm in D-D″ and insets in G.

injection site in the dorsal striatum, BrdU$^+$/GFP$^+$ cells were not observed in other regions of the striatum or of the IC and EC. Collectively, these data indicate that most newborn DCX$^+$ cells in the EC-LS are transient elements that retain the expression of DCX throughout their existence.

Interestingly, 72±12% of the DCX staining in the EC-LS was located within the white matter tract of IC or EC. Conversely, a 3D reconstruction of 23 randomly chosen IC bundles located within 300 µm of the EC in a p18 animal indicated that 16 (70%) of them contained DCX$^+$ processes for more than 80% of their length. Serial section 3D reconstructions of DCX$^+$ cells in these IC bundles revealed that most of these cells have complex morphologies with some of their processes extending over a millimeter (Fig. 11I-L; supplementary material Movie 1). In general, the morphology of the DCX$^+$ cells in the EC, LS and IC did not match that of any known striatal cell type, supporting the proposal that these cells represent previously undescribed cell types, the function of which remains to be investigated. Interestingly, almost all EC-LS individual DCX$^+$ cells expressed Sp8 (Fig. 11D), a transcription factor that is associated with distinct lateral and caudal ganglionic eminence-derived interneurons (Ma et al., 2012; Waclaw et al., 2006).

DISCUSSION

Here we demonstrate that the LS of the guinea pig contains a population of NPs that is quiescent at birth and becomes transiently activated during juvenile life, giving rise to neuroblasts that are characterized by a transient existence.

Activation of quiescent NPs

The occurrence of quiescent NPs within the adult brain parenchyma has long been hypothesized (Emsley et al., 2005; Ourednik et al., 2001; Palmer et al., 1999). Here, we provide clear evidence that such cells can actually occur *in vivo* and can be activated under normal conditions. By coupling a viral lineage tracing with BrdU labeling, we directly proved that new EC-LS neuroblasts are generated locally from progenitors that already reside in the EC-LS at birth but become activated only later in postnatal development. Intraventricular injections of the VSVG-GFP did not reveal any contribution of the SVZ to the EC-LS neurogenic system. Thus, although we cannot exclude the possibility that a small population of spatially restricted SVZ progenitors was spared from our viral injections, these results support the notion that local NPs are the major, if not unique, source of EC-LS neuroblasts.

Our analyses strongly suggest that EC-LS NPs are located in the vPSB, where, around weaning, we observed the appearance of a germinative-like layer showing chains of neuroblasts closely associated with clusters of intermediate-like progenitors. The vPSB was also enriched in astrocytes that, as the primary NPs of constitutive neurogenic niches, express immature markers, proliferate at a low rate and retain BrdU labeling in the long-term (Doetsch et al., 1999; Lugert et al., 2010; Ponti et al., 2013). These cells were also preferentially labeled by VSVG-GFP at birth, further supporting that the primary NPs of the vPSB are BLBP$^+$ astrocytes. This idea is consistent with the fact that both embryonic and adult primary NPs are within the astroglial lineage (Doetsch et al., 1999; Anthony et al.,

Development (2014) 141, 4065-4075 doi:10.1242/dev.107987

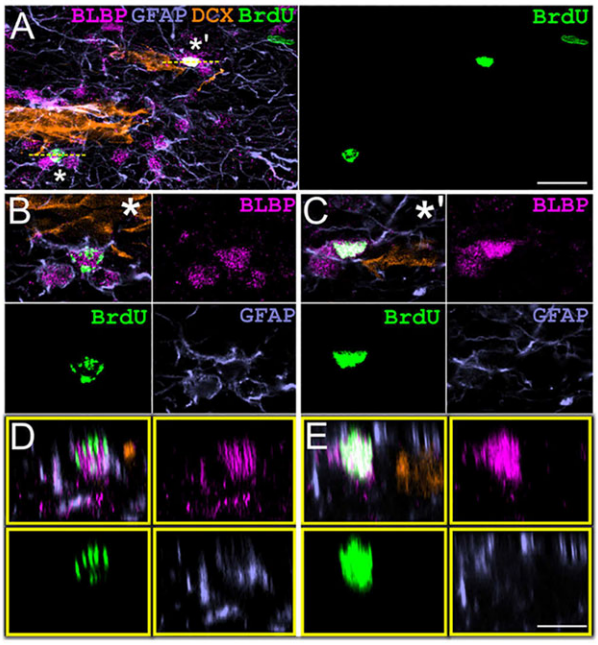

Fig. 6. BLBP$^+$ cells are label-retaining cells. (A) *z*-projection of the vPSB in a p65 animal showing two label-retaining cells (marked by asterisk and asterisk with prime) stained for BLBP (magenta) and BrdU (green), and surrounded by GFAP$^+$ processes. (B-E) Single confocal plane along the lines in A (B,C) and reslice (D,E) showing a clear colocalization with GFAP (asterisk) and a more ambiguous colocalization (asterisk with prime). Scale bars: 20 µm in A; 10 µm in B-E.

2004). Although parenchymal astrocytes have not yet been shown to produce neurons in the adult brain, acute lesions can stimulate a neurogenic potential in these cells, at least *in vitro* (Buffo et al., 2008; Sirko et al., 2013). Together with our results, one interpretation of these data is that some parenchymal astrocytes possess a physiological neurogenic potential that requires specific cues in order to be activated. It is of note that, in respect to other EC-LS regions, the vPSB of newborn animals showed a relatively high level of proliferation and contained a few BLBP/Ki67$^+$ cells. Accordingly, BrdU injections at birth resulted in a few BrdU-labeled neuroblasts at p12. This might indicate that the vPSB is not entirely quiescent at birth, but rather that some rare EC-LS progenitors are either already activated or undergo non-neurogenic cell division.

The ability to switch between active and quiescent states is a fundamental feature of adult stem cells, including the neurogenic astrocytes of the SVZ and DG (Cheung and Rando, 2013; Wang et al., 2011). These cells operate within neurogenic niches that are set during embryonic development and are thought to play an active role in regulating their quiescence and their capacity to produce neurons (Fuentealba et al., 2012; Kriegstein and Alvarez-Buylla, 2009). In this respect, the activation of vPSB progenitors is particularly surprising as it occurs within a tissue that is classically considered strongly gliogenic (Emsley et al., 2005; Ninkovic and Götz, 2013). This latter concept, however, is mainly derived from heterotopic transplantation of NPs (Eriksson et al., 2003; Lim et al., 2000; Shihabuddin et al., 2000) and it should not be generalized. Accordingly, a few cases of parenchymal NPs are emerging (Bi et al., 2011; Luzzati et al., 2006, 2011a; Ohira et al., 2010; Ponti et al., 2008) and here we provide an unequivocal example that such cells can eventually give rise to a germinative-like layer. The next step will be to understand how quiescent parenchymal NPs are activated in the adult brain as well as the cues that sustain their ability to produce neurons *in vivo*.

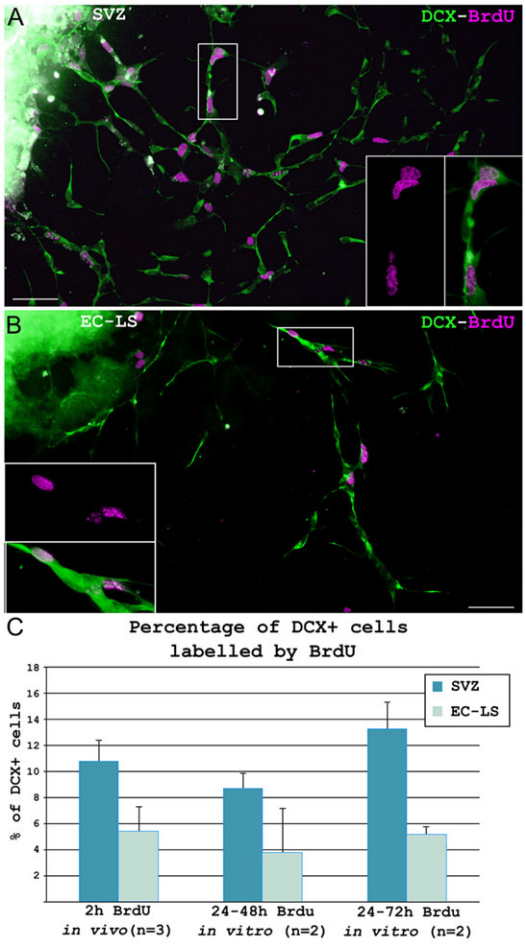

Fig. 7. Tissue explants from BrdU-treated animals. (A,B) SVZ (A) and EC-LS (B) tissue explants grown in culture for 3 days were obtained from a p18 animal that received a BrdU injection 2 h before sacrifice. Explants are labeled for DCX (green) and BrdU (magenta). Insets show higher magnifications. (C) The percentage of DCX$^+$ cells labeled by BrdU in the SVZ or EC-LS when the BrdU is given *in vivo* (2 h) or *in vitro* between 24 and 48 h or 24 and 72 h after plating. Error bars indicate s.d. Scale bars: 20 µm.

Fate of the newly generated neuroblasts

Although quiescent parenchymal NPs represent an attractive new source of neurons for endogenous repair, understanding their specification remains a fundamental issue. Newborn DCX$^+$ cells in the EC-LS exist transiently and do not express markers of either mature or immature striatal cell types. Nonetheless, these cells often show differentiated morphologies. It is noteworthy that an elevated death rate of newly generated neurons is a common feature in different studies of striatal and cortical neurogenesis, in both normal and pathologic conditions (Arvidsson et al., 2002; Chen et al., 2004; Gould et al., 2001; Luzzati et al., 2006, 2011a). The death of new striatal and cortical neurons has often been attributed to a strong selection exerted by a non-permissive environment (Kernie and Parent, 2010). This hypothesis is not, however, consistent with data showing that transplanted embryonic precursors can survive and differentiate within the adult striatum and neocortex (Luzzati et al., 2011a; Shin et al., 2000). Rather, transient neurons have been described during embryonic development and early postnatal stages (Niquille et al., 2009; Teissier et al., 2012) and, at least in the neocortex, it has been suggested that their death is regulated by intrinsically defined mechanisms (Southwell et al., 2012).

Development (2014) 141, 4065-4075 doi:10.1242/dev.107987

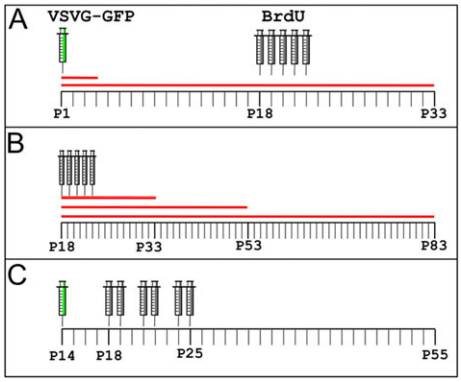

Fig. 8. Experimental design for analysis of the origin and fate of EC-LS neurons. (A) Lineage tracing of EC-LS and SVZ cells before the activation of neurogenesis. (B) Timecourse of newborn neuron survival and differentiation. (C) Fate of virally tagged newborn neurons. Red lines indicate survival time.

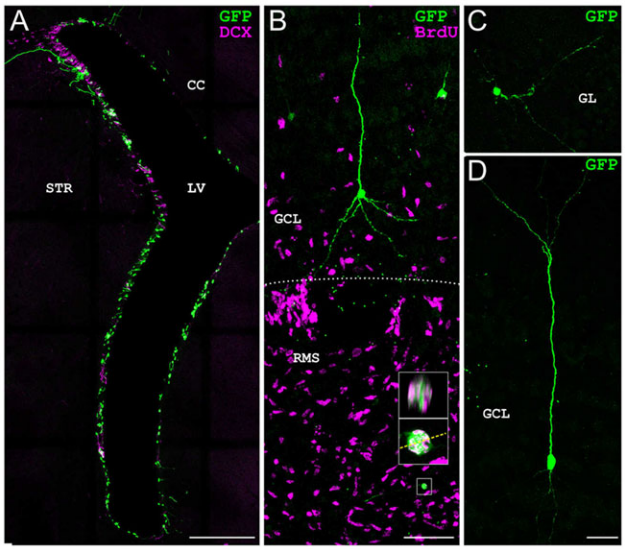

Fig. 9. Viral lineage tracing of SVZ progenitors. (A) GFP (green) and DCX (magenta) staining in the SVZ at the level of the lateral ventricle of a p33 animal. (B) BrdU$^+$ (magenta) and GFP$^+$ (green) cells in the deep granule cell layer and RMS of a p33 animal. Insets show a higher magnification and a reslice of a BrdU$^+$/GFP$^+$ cell. Dotted line indicates the border between RMS and GCL. (C,D) GFP-labeled periglomerular (C) and upper (D) granule cell. CC, corpus callosum; GCL, granule cell layer; GL, glomerular layer; LV, lateral ventricle; STR, striatum; RMS, rostral migratory stream. Scale bars. 400 µm in A; 100 µm in B; 50 µm in C,D.

Interestingly, these cells are often directed to white matter tracts, where they contribute to the guidance of growing axons (López-Bendito et al., 2006; Niquille et al., 2009, 2013; Sato et al., 1998). Moreover, these cells originate, in part, from the caudal ganglionic eminence, a major source of Sp8$^+$ interneurons (Ma et al., 2012; Niquille et al., 2013). These observations raise the possibility that the transient EC-LS neuroblasts belong to a broader population of cells involved in transient forms of plasticity, possibly related to the remodeling of long-range connections. Additional analyses will be required to test this hypothesis.

Similarities between EC-LS and lesion-induced neurogenic systems

Striatal neurogenesis has been described in different mammalian species in both normal and pathologic conditions (Bédard et al., 2002; Luzzati et al., 2006, 2011a; Tattersfield et al., 2004). The organization of the vPSB is consistently different from the scattered and PAX6-negative clusters of proliferating cells that we observed in the striatal gray matter of the rabbit and of a mice

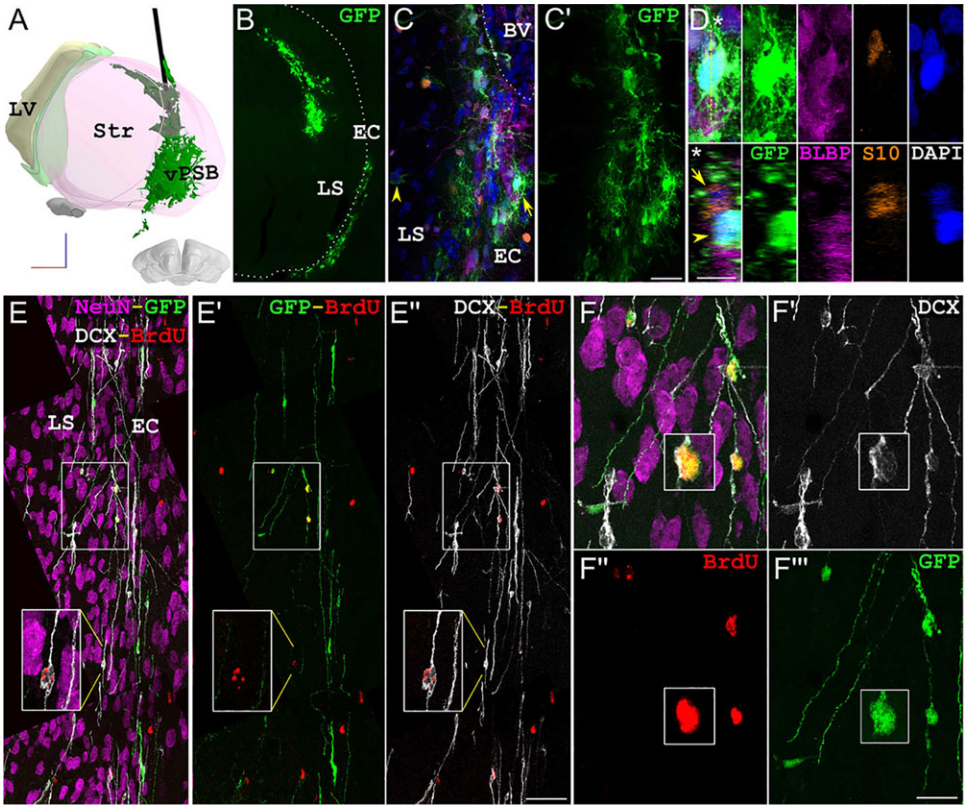

Fig. 10. Viral lineage tracing of EC-LS progenitors. (A) Frontal views of a 3D model of GFP staining in the striatum of a p4 animal injected with VSVG-GFP at p1. The needle track is in black; GFP staining is dark green within the striatum and light green outside. (B) GFP staining (green) in a section at the level of the injection site. (C,C′) The vPSB at p4 stained for GFP (green), BLBP (magenta), SOX10 (orange) and with DAPI (blue). Arrowhead indicates a GFP$^+$ cell in the LS. (D) *z*-projection and reslice (asterisk) of the BLBP$^+$/GFP$^+$ cell indicated by an arrow in C. (E-F‴) Dorsal EC-LS of a p33 animal labeled for GFP (green), DCX (white), BrdU (red) and NeuN (magenta). The inset in E-E″ shows a DCX$^+$/BrdU$^+$ but GFP$^-$ cell. (F-F‴) Higher magnification of the area outlined in E-E″ showing three cells triple labeled for DCX, BrdU and GFP (one cell is magnified in the inset). Scale bars: 200 µm in B; 50 µm in E-E″; 40 µm in C,C′; 20 µm in F.

Development (2014) 141, 4065-4075 doi:10.1242/dev.107987

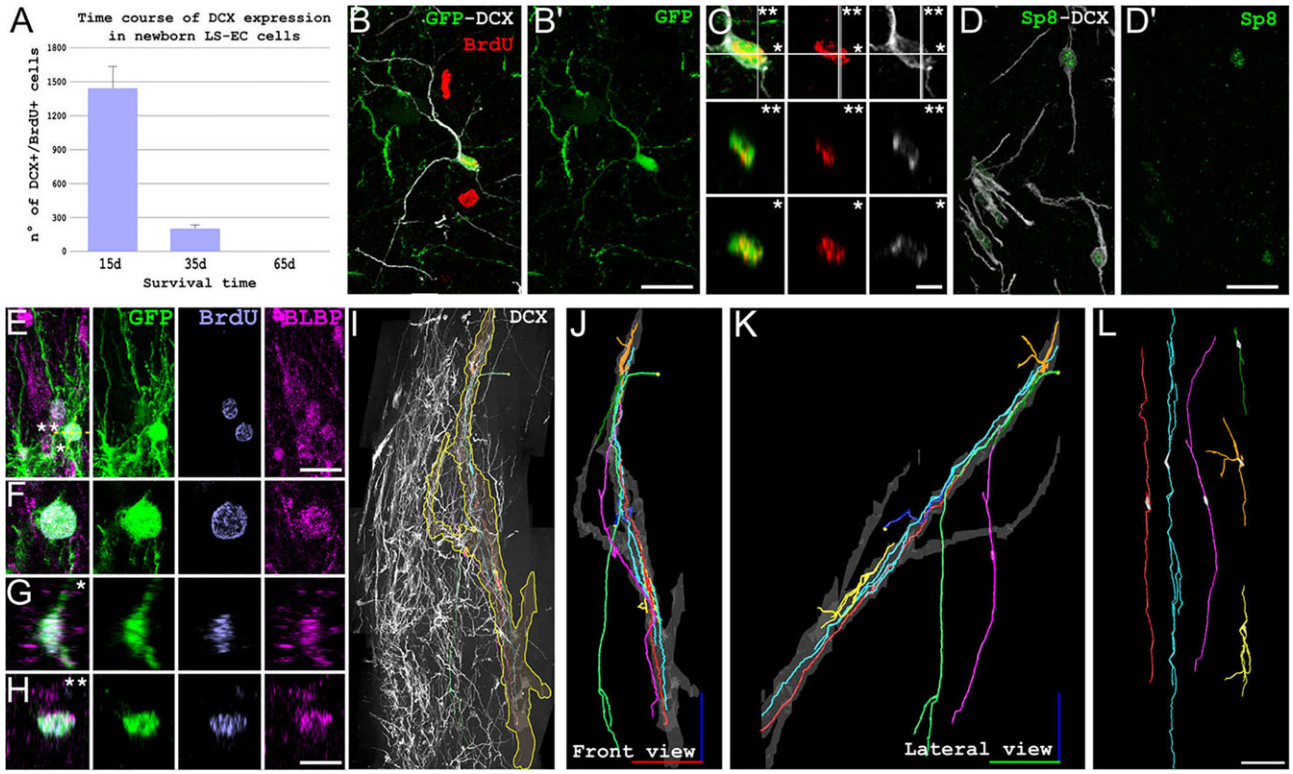

Fig. 11. Fate of the newly generated EC-LS neuroblasts. (A) Timecourse of the number of DCX/BrdU double-labeled cells in the EC-LS. Error bars indicate s.d. (B,B′) One cell in the LS of an animal treated as shown in Fig. 8C, triple labeled for DCX (white), GFP (green) and BrdU (red). (C) Higher magnification of the cell body of the cell in B; single and double asterisks are reslices along the indicated planes. (D,D′) DCX^+ cells (white) in the LS expressing Sp8 (green). (E-H) *z*-projection (E), single slice (F) and reslices (G,H) of a cell labeled for GFP (green), BLBP (magenta) and BrdU (violet) in an animal treated as shown in Fig. 8C. (I) *z*-projection of a 3D reconstructed tract of 750 µm of the dorsal EC-LS stained for DCX. (J-L) Reconstruction of an IC bundle (traced on the basis of the MAG staining; yellow outline in I, gray shade in J,K), and of all the DCX^+ cells and processes contacting it (colored lines). Some cells have the cell body outside the IC bundle (blue, magenta and light green). The small yellow spheres indicate processes exiting outside the reconstructed volume (blue and light green). (L) Individual views of the reconstructed cells. Scale bars: 100 µm in I-L; 20 µm in B,B′,D-E; 10 µm in C,F-H.

model of progressive degeneration (Luzzati et al., 2006). Rather, the vPSB is more closely related to the SVZ and, in particular, with its lateral extension along the dorsal pallial subpallial boundary (dPSB) (Luzzati et al., 2011a). We previously showed that the mouse dPSB is strongly expanded during progressive degeneration and is the main source of neuroblasts directed to the striatum. These cells share several features with the EC-LS neuroblasts, including the expression of Sp8, a transient existence and the tropism for IC bundles. Since DCX^+ cells are not observed in the EC-LS of rabbits and mice (F.L., unpublished observation), we cannot exclude the possibility that the postnatal EC-LS neurogenic system is specific to the guinea pig, possibly related to the highly precocial nature of this species. Nonetheless, its precise spatial and temporal regulation makes the vPSB an ideal model with which to study the activation of quiescent progenitors as well as the role of parenchymal neurogenesis in the striatum. In this respect, this model might also shed new light on the role of lesion-induced neurogenesis.

MATERIALS AND METHODS

Animals, BrdU injections and tissue preparation

All experimental procedures were in accordance with the European Communities Council Directive of 24 November 1986 (86 609 EEC), the Italian law for the care and use of experimental animals (DL116 92) and approved by the Italian Ministry of Health and the Bioethical Committee of the University of Turin. All experiments were designed to minimize the numbers of animals used and their discomfort.

Experiments were performed on 88 male and female Hartley guinea pigs (*Cavia porcellus*) ranging from birth to 8 months of age. Forty-one animals were intraperitoneally injected with 5-bromo-2-deoxyuridine (BrdU; Sigma; 50 mg/kg body weight in 0.1 M Tris pH 7.6). Animals were deeply anesthetized with a ketamine/xylazine solution (100 and 33 mg/kg, respectively) and transcardially perfused with an ice-cold saline solution (0.9% NaCl), followed by a solution of 4% paraformaldehyde (PFA) plus 2% picric acid in 0.1 M sodium phosphate buffer. Brains were then postfixed overnight, cryoprotected, frozen at −80°C, and cut on a cryostat in series of 40 or 50 µm thick coronal sections.

Electron microscopy

p18 guinea pigs were perfused intracardially with an heparinized saline solution followed by 2% glutaraldehyde plus 1% PFA in 0.1 M sodium phosphate buffer pH 7.4. Brains were postfixed for 2 h and cut coronally with a Vibratome (300 µm slices). Sections were fixed in osmium ferrocyanide for 1 h, stained with 1% uranyl acetate, dehydrated and embedded in Araldite. Ultra-thin sections were examined under a JEM-1010 transmission electron microscope (Jeol) equipped with a side-mounted CCD camera (Mega View III; Soft Imaging Systems) for photography.

Lentiviral vectors

Vector stocks were produced by transient transfection of the transfer plasmid expressing eGFP under the control of the CMV promoter, the packaging plasmids pMDLg/pRRE and pRSV.REV, and the VSV envelope plasmid pMD2.VSV-G in 293T cells as described (Follenzi et al., 2000). Viral particles were purified and concentrated by ultracentrifugation as described (Dull et al., 1998). Vector titer on HeLa cells was 2×10^9 TU/ml. The virus was then diluted 1/20 in PBS containing 0.6% glucose and frozen at −80°C.

Development (2014) 141, 4065-4075 doi:10.1242/dev.107987

Stereotaxic injections

Animals were anesthetized by intraperitoneal injection of ketamine (30 mg/kg; Ketavet; Bayer) supplemented with xylazine (3 mg/kg; Rompun; Bayer) and positioned in a stereotaxic apparatus (Stoelting). Using a glass micropipette and a pneumatic pressure injection apparatus (Picospritzer II; General Valve Corp), 3 µl of VSVG-GFP was bilaterally injected at stereotaxic coordinates 2 mm AP, ±2 mm ML and −4 mm DV; 2 µl of the VSVG-GFP virus were injected at stereotaxic coordinates 1.5 mm AP, ±5 mm ML and −5 mm DV.

Organotypic cultures

Tissue explant cultures were performed as described by Garzotto et al. (2008). Briefly, brains were dissected out and cut by Vibratome into 250 µm thick coronal slices. Tissues from SVZ and vPSB were trimmed into pieces of ∼300 µm. Explants were subsequently embedded in 75% Matrigel growth factor reduced (BD Biosciences). Explants were maintained 3 days *in vitro* in 5% CO_2 at 37°C in Neurobasal medium (Invitrogen) supplemented with 1× N-2 (Invitrogen), 25 µg/ml gentamicin (Invitrogen) and 0.5 mM glutamine (Invitrogen). BrdU (10 µM) was added to the culture medium of some explants on the first or second day *in vitro*.

Immunohistochemistry

Immunohistochemical reactions were performed on sections incubated for 24-48 h at 4°C in a solution of 0.01 M PBS (pH 7.4) containing 0.5-1% Triton X-100, normal serum and primary antibodies (supplementary material Table S1). For BrdU staining, DNA was denatured in 2 N HCl for 30 min at 37°C. Sections were then rinsed in 0.1 M borate buffer (pH 8.5). Sections were then incubated with appropriate solutions of secondary antisera (supplementary material Table S1). Slides were coverslipped with antifade mounting medium with DABCO (Sigma) and analyzed with a laser scanning TCS SP5 (Leica Microsystems). Images were processed using ImageJ (NIH) and Photoshop 7.0 (Adobe Systems). Only whole-image adjustments to color, contrast and brightness were made.

Light and confocal 3D reconstructions

3D reconstructions were performed as described by Luzzati et al. (2011a,b). Briefly, images from each section were stitched in Fiji (http://fiji.sc/Image_Stitching), aligned, traced and rendered in Reconstruct 1.1 (http://synapses.clm.utexas.edu/tools/reconstruct/reconstruct.stm). The entire EC-LS 3D reconstruction at p18 was performed on 165 40 µm thick coronal sections (voxel size 0.76×0.76×40 µm). The reconstruction of the vPSB chains, IC bundles (voxel size 0.76×0.76×2 µm) and DCX^+ cells in an IC bundle (voxel size 0.12×0.12×0.8 µm) was performed on 15 consecutive 50 µm thick sections. For reconstruction of DCX^+ cells, the IC was traced in Reconstruct and DCX^+ cells in Neuronstudio 1.6 (Darren Myatt, University of Reading, UK). The two reconstructions were fused in Blender 2.6 (Blender Foundation, Amsterdam, The Netherlands). Texturing and rendering of the 3D models was performed in Blender.

Quantifications and statistical analyses

The total number of cells was evaluated stereologically either with Neurolucida 7.0 (MBF Bioscience) (DCX^+ and $DCX^+/Ki67^+$) or by confocal microscope ($DCX^+/BrdU^+$) in a one-in-six series of sections (40 µm thick).

The density of $BrdU^+$ and $Ki67^+$ cells was evaluated in ImageJ in three to five confocal sections (n=3; voxel size 0.38×0.38×1 µm). For the LS we considered the area located within the first 300 µm lateral to the EC. Cells counted per animal ranged 38-110 for $BrdU^+$, 108-363 for $Ki67^+$, 0-12 for $BLBP^+/Ki67^+$ and 5-12 for $BLBP^+/BrdU^+$ cells in the vPSB.

The percentage of cells in $KI67^+$ clusters (defined as a group of at least four cells with closely contacting cell bodies) that expressed DCX was evaluated by counting 137-170 cells per animal using a confocal microscope (voxel size 0.38×0.38×1 µm). The percentage of DCX^+ cells in $Ki67^+$ clusters was counted on 24 clusters per animal (n=3). Percentage of KaD, $Ki67^+/DCX^+$ and $Ki67^-/DCX^+$ cells colabeled for PAX6 and SOX9 was evaluated in 80-126 cells per animal for each cell type.

The percentage of DCX^+ cells colabeled for GFP and BrdU in the LS and dorsal EC was counted in Fiji in 50 µm thick sections spaced 300 µm apart, acquired at the confocal microscope (voxel size 0.38×0.38×1 µm). For the lineage tracing of vPSB progenitors, in each animal a minimum of three sections and 30 GFP^+/DCX^+ cells were counted. For the fate of virally tagged newborn neurons, all sections were counted.

The total number of cells that had migrated from *in vitro* explants was manually counted with Neurolucida 7.0.

Statistical analyses were performed using Statistical Package for the Social Sciences 14.0 (SPSS). Analysis of variance (ANOVA) was followed by Tukey's post-hoc test when appropriate.

Acknowledgements

We thank Andrea Moscato and Monica Masciavè for their important contribution to the preliminary set of experiments of this work. This work is dedicated to the memory of Professor Maria Fosca Franzoni.

Competing interests

The authors declare no competing financial interests.

Author contributions

F.L. designed and performed the experiments, analyzed the data and wrote the paper. P.P. assisted in experiment design, data analysis and writing. A.F. assisted in the experimental design. M.A. and L.B. performed the electron microscopy. E.V. and C.R. produced the viral vector. G.N. and L.O. assisted in the acquisition and analysis of data.

Funding

This work was supported by PRIN-Peretto 2010-2011.

Supplementary material

Supplementary material available online at
http://dev.biologists.org/lookup/suppl/doi:10.1242/dev.107987/-/DC1

References

Anthony, T. E., Klein, C., Fishell, G. and Heintz, N. (2004). Radial glia serve as neuronal progenitors in all regions of the central nervous system. *Neuron* **41**, 881-890.

Arvidsson, A., Collin, T., Kirik, D., Kokaia, Z. and Lindvall, O. (2002). Neuronal replacement from endogenous precursors in the adult brain after stroke. *Nat. Med.* **8**, 963-970.

Bédard, A., Cossette, M., Lévesque, M. and Parent, A. (2002). Proliferating cells can differentiate into neurons in the striatum of normal adult monkey. *Neurosci. Lett.* **328**, 213-216.

Bi, B., Salmaso, N., Komitova, M., Simonini, M. V., Silbereis, J., Cheng, E., Kim, J., Luft, S., Ment, L. R., Horvath, T. L. et al. (2011). Cortical glial fibrillary acidic protein-positive cells generate neurons after perinatal hypoxic injury. *J. Neurosci.* **31**, 9205-9221.

Bonfanti, L. and Peretto, P. (2011). Adult neurogenesis in mammals–a theme with many variations. *Eur. J. Neurosci.* **34**, 930-950.

Buffo, A., Rite, I., Tripathi, P., Lepier, A., Colak, D., Horn, A.-P., Mori, T. and Gotz, M. (2008). Origin and progeny of reactive gliosis: a source of multipotent cells in the injured brain. *Proc. Natl. Acad. Sci. USA* **105**, 3581-3586.

Chen, J., Magavi, S. S. P. and Macklis, J. D. (2004). Neurogenesis of corticospinal motor neurons extending spinal projections in adult mice. *Proc. Natl. Acad. Sci. USA* **101**, 16357-16362.

Cheng, L.-C., Pastrana, E., Tavazoie, M. and Doetsch, F. (2009). miR-124 regulates adult neurogenesis in the subventricular zone stem cell niche. *Nat. Neurosci.* **12**, 399-408.

Cheung, T. H. and Rando, T. A. (2013). Molecular regulation of stem cell quiescence. *Nat. Rev. Mol. Cell Biol.* **14**, 329-340.

Dayer, A. G., Cleaver, K. M., Abouantoun, T. and Cameron, H. A. (2005). New GABAergic interneurons in the adult neocortex and striatum are generated from different precursors. *J. Cell Biol.* **168**, 415-427.

Doetsch, F., Caillé, I., Lim, D. A., García-Verdugo, J. M. and Alvarez-Buylla, A. (1999). Subventricular zone astrocytes are neural stem cells in the adult mammalian brain. *Cell* **97**, 703-716.

Dull, T., Zufferey, R., Kelly, M., Mandel, R. J., Nguyen, M., Trono, D. and Naldini, L. (1998). A third-generation lentivirus vector with a conditional packaging system. *J. Virol.* **72**, 8463-8471.

Emsley, J. G., Mitchell, B. D., Kempermann, G. and Macklis, J. D. (2005). Adult neurogenesis and repair of the adult CNS with neural progenitors, precursors, and stem cells. *Prog. Neurobiol.* **75**, 321-341.

Eriksson, C., Björklund, A. and Wictorin, K. (2003). Neuronal differentiation following transplantation of expanded mouse neurosphere cultures derived from different embryonic forebrain regions. *Exp. Neurol.* **184**, 615-635.

Follenzi, A., Ailles, L. E., Bakovic, S., Geuna, M. and Naldini, L. (2000). Gene transfer by lentiviral vectors is limited by nuclear translocation and rescued by HIV-1 pol sequences. *Nat. Genet.* **25**, 217-222.
Fuentealba, L. C., Obernier, K. and Alvarez-Buylla, A. (2012). Adult neural stem cells bridge their niche. *Cell Stem Cell* **10**, 698-708.
Garcia, A. D. R., Doan, N. B., Imura, T., Bush, T. G. and Sofroniew, M. V. (2004). GFAP-expressing progenitors are the principal source of constitutive neurogenesis in adult mouse forebrain. *Nat. Neurosci.* **7**, 1233-1241.
Garzotto, D., Giacobini, P., Crepaldi, T., Fasolo, A. and De Marchis, S. (2008). Hepatocyte growth factor regulates migration of olfactory interneuron precursors in the rostral migratory stream through Met-Grb2 coupling. *J. Neurosci.* **28**, 5901-5909.
Giachino, C., Basak, O., Lugert, S., Knuckles, P., Obernier, K., Fiorelli, R., Frank, S., Raineteau, O., Alvarez-Buylla, A. and Taylor, V. (2013). Molecular diversity subdivides the adult forebrain neural stem cell population. *Stem Cells* 32, 70-84.
Götz, M., Stoykova, A. and Gruss, P. (1998). Pax6 controls radial glia differentiation in the cerebral cortex. *Neuron* **21**, 1031-1044.
Gould, E., Vail, N., Wagers, M. and Gross, C. G. (2001). Adult-generated hippocampal and neocortical neurons in macaques have a transient existence. *Proc. Natl. Acad. Sci. USA* **98**, 10910-10917.
Hack, M. A., Saghatelyan, A., de Chevigny, A., Pfeifer, A., Ashery-Padan, R., Lledo, P.-M. and Götz, M. (2005). Neuronal fate determinants of adult olfactory bulb neurogenesis. *Nat. Neurosci.* **8**, 865-872.
Kawaguchi, Y. (1997). Neostriatal cell subtypes and their functional roles. *Neurosci. Res.* **27**, 1-8.
Kernie, S. G. and Parent, J. M. (2010). Forebrain neurogenesis after focal Ischemic and traumatic brain injury. *Neurobiol. Dis.* **37**, 267-274.
Kohwi, M., Osumi, N., Rubenstein, J. L. R. and Alvarez-Buylla, A. (2005). Pax6 is required for making specific subpopulations of granule and periglomerular neurons in the olfactory bulb. *J. Neurosci.* **25**, 6997-7003.
Kriegstein, A. and Alvarez-Buylla, A. (2009). The glial nature of embryonic and adult neural stem cells. *Annu. Rev. Neurosci.* **32**, 149-184.
Künkele, J. and Trillmich, F. (1997) Are precocial young cheaper? Lactation energetics in the guinea pig. *Physiol. Zool.* **70**, 589-596.
Le Magueresse, C., Alfonso, J., Khodosevich, K., Arroyo Martín, A. A., Bark, C. and Monyer, H. (2011). "Small axonless neurons": postnatally generated neocortical interneurons with delayed functional maturation. *J. Neurosci.* **31**, 16731-16747.
Lim, D. A., Tramontin, A. D., Trevejo, J. M., Herrera, D. G., García-Verdugo, J. M. and Alvarez-Buylla, A. (2000). Noggin antagonizes BMP signaling to create a niche for adult neurogenesis. *Neuron* **28**, 713-726.
Liu, F., You, Y., Li, X., Ma, T., Nie, Y., Wei, B., Li, T., Lin, H. and Yang, Z. (2009). Brain injury does not alter the intrinsic differentiation potential of adult neuroblasts. *J. Neurosci.* **29**, 5075-5087.
Lois, C. and Alvarez-Buylla, A. (1993). Proliferating subventricular zone cells in the adult mammalian forebrain can differentiate into neurons and glia. *Proc. Natl. Acad. Sci. USA* **90**, 2074-2077.
López-Bendito, G., Cautinat, A., Sánchez, J. A., Bielle, F., Flames, N., Garratt, A. N., Talmage, D. A., Role, L. W., Charnay, P., Marín, O. et al. (2006). Tangential neuronal migration controls axon guidance: a role for neuregulin-1 in thalamocortical axon navigation. *Cell* **125**, 127-142.
Lugert, S., Basak, O., Knuckles, P., Haussler, U., Fabel, K., Götz, M., Haas, C. A., Kempermann, G., Taylor, V. and Giachino, C. (2010). Quiescent and active hippocampal neural stem cells with distinct morphologies respond selectively to physiological and pathological stimuli and aging. *Cell Stem Cell* **6**, 445-456.
Luzzati, F., De Marchis, S., Fasolo, A. and Peretto, P. (2006). Neurogenesis in the caudate nucleus of the adult rabbit. *J. Neurosci.* **26**, 609-621.
Luzzati, F., De Marchis, S., Parlato, R., Gribaudo, S., Schütz, G., Fasolo, A. and Peretto, P. (2011a). New striatal neurons in a mouse model of progressive striatal degeneration are generated in both the subventricular zone and the striatal parenchyma. *PLoS ONE* **6**, e25088.
Luzzati, F., Fasolo, A. and Peretto, P. (2011b). Combining confocal laser scanning microscopy with serial section reconstruction in the study of adult neurogenesis. *Front. Neurosci.* **5**, 70.
Ma, T., Zhang, Q., Cai, Y., You, Y., Rubenstein, J. L. R. and Yang, Z. (2012). A subpopulation of dorsal lateral/caudal ganglionic eminence-derived neocortical interneurons expresses the transcription factor Sp8. *Cereb. Cortex* **22**, 2120-2130.
Maekawa, M., Takashima, N., Arai, Y., Nomura, T., Inokuchi, K., Yuasa, S. and Osumi, N. (2005). Pax6 is required for production and maintenance of progenitor cells in postnatal hippocampal neurogenesis. *Genes Cells* **10**, 1001-1014.
Marin, O., Anderson, S. A. and Rubenstein, J. L. (2000). Origin and molecular specification of striatal interneurons. *J. Neurosci.* **20**, 6063-6076.
Merkle, F. T., Mirzadeh, Z. and Alvarez-Buylla, A. (2007). Mosaic organization of neural stem cells in the adult brain. *Science* **317**, 381-384.
Ming, G.-L. and Song, H. (2011). Adult neurogenesis in the mammalian brain: significant answers and significant questions. *Neuron* **70**, 687-702.
Ninkovic, J. and Götz, M. (2013). Fate specification in the adult brain–lessons for eliciting neurogenesis from glial cells. *BioEssays* **35**, 242-252.
Niquille, M., Garel, S., Mann, F., Hornung, J.-P., Otsmane, B., Chevalley, S., Parras, C., Guillemot, F., Gaspar, P., Yanagawa, Y. et al. (2009). Transient neuronal populations are required to guide callosal axons: a role for semaphorin 3C. *PLoS Biol.* **7**, e1000230.
Niquille, M., Minocha, S., Hornung, J.-P., Rufer, N., Valloton, D., Kessaris, N., Alfonsi, F., Vitalis, T., Yanagawa, Y., Devenoges, C. et al. (2013). Two specific populations of GABAergic neurons originating from the medial and the caudal ganglionic eminences aid in proper navigation of callosal axons. *Dev. Neurobiol.* **73**, 647-672.
Ohira, K., Furuta, T., Hioki, H., Nakamura, K. C., Kuramoto, E., Tanaka, Y., Funatsu, N., Shimizu, K., Oishi, T., Hayashi, M. et al. (2010). Ischemia-induced neurogenesis of neocortical layer 1 progenitor cells. *Nat. Neurosci.* **13**, 173-179.
Ourednik, V., Ourednik, J., Flax, J. D., Zawada, W. M., Hutt, C., Yang, C., Park, K. I., Kim, S. U., Sidman, R. L., Freed, C. R. et al. (2001). Segregation of human neural stem cells in the developing primate forebrain. *Science* **293**, 1820-1824.
Palmer, T. D., Markakis, E. A., Willhoite, A. R., Safar, F. and Gage, F. H. (1999). Fibroblast growth factor-2 activates a latent neurogenic program in neural stem cells from diverse regions of the adult CNS. *J. Neurosci.* **19**, 8487-8497.
Ponti, G., Peretto, P. and Bonfanti, L. (2008). Genesis of neuronal and glial progenitors in the cerebellar cortex of peripuberal and adult rabbits. *PLoS ONE* **3**, e2366.
Ponti, G., Obernier, K., Guinto, C., Jose, L., Bonfanti, L. and Alvarez-Buylla, A. (2013). Cell cycle and lineage progression of neural progenitors in the ventricular-subventricular zones of adult mice. *Proc. Natl. Acad. Sci. USA* **110**, E1045-E1054.
Sato, Y., Hirata, T., Ogawa, M. and Fujisawa, H. (1998). Requirement for early-generated neurons recognized by monoclonal antibody Lot1 in the formation of lateral olfactory tract. *J. Neurosci.* **18**, 7800-7810.
Schnitzer, J., Franke, W. W. and Schachner, M. (1981). Immunocytochemical demonstration of vimentin in astrocytes and ependymal cells of developing and adult mouse nervous system. *J. Cell Biol.* **90**, 435-447.
Scholzen, T. and Gerdes, J. (2000). The Ki-67 protein: from the known and the unknown. *J. Cell. Physiol.* **182**, 311-322.
Shihabuddin, L. S., Horner, P. J., Ray, J. and Gage, F. H. (2000). Adult spinal cord stem cells generate neurons after transplantation in the adult dentate gyrus. *J. Neurosci.* **20**, 8727-8735.
Shin, J. J., Fricker-Gates, R. A., Perez, F. A., Leavitt, B. R., Zurakowski, D. and Macklis, J. D. (2000). Transplanted neuroblasts differentiate appropriately into projection neurons with correct neurotransmitter and receptor phenotype in neocortex undergoing targeted projection neuron degeneration. *J. Neurosci.* **20**, 7404-7416.
Sirko, S., Behrendt, G., Johansson, P. A., Tripathi, P., Costa, M. R., Bek, S., Heinrich, C., Tiedt, S., Colak, D., Dichgans, M. et al. (2013). Reactive glia in the injured brain acquire stem cell properties in response to sonic hedgehog. *Cell Stem Cell* **12**, 426-439.
Southwell, D. G., Paredes, M. F., Galvao, R. P., Jones, D. L., Froemke, R. C., Sebe, J. Y., Alfaro-Cervello, C., Tang, Y., Garcia-Verdugo, J. M., Rubenstein, J. L. et al. (2012). Intrinsically determined cell death of developing cortical interneurons. *Nature* **491**, 109-113.
Tattersfield, A. S., Croon, R. J., Liu, Y. W., Kells, A. P., Faull, R. L. M. and Connor, B. (2004). Neurogenesis in the striatum of the quinolinic acid lesion model of Huntington's disease. *Neuroscience* **127**, 319-332.
Teissier, A., Waclaw, R. R., Griveau, A., Campbell, K. and Pierani, A. (2012). Tangentially migrating transient glutamatergic neurons control neurogenesis and maintenance of cerebral cortical progenitor pools. *Cereb. Cortex* **22**, 403-416.
Waclaw, R. R., Allen, Z. J., Bell, S. M., Erdélyi, F., Szabó, G., Potter, S. S. and Campbell, K. (2006). The zinc finger transcription factor Sp8 regulates the generation and diversity of olfactory bulb interneurons. *Neuron* **49**, 503-516.
Wang, Y.-Z., Plane, J. M., Jiang, P., Zhou, C. J. and Deng, W. (2011). Concise review: quiescent and active states of endogenous adult neural stem cells: identification and characterization. *Stem Cells* **29**, 907-912.